CARBON 52 (2013) 356–362

Available at www.sciencedirect.com

SciVerse ScienceDirect

journal homepage: www.elsevier.com/locate/carbon

Macroscopic self-standing SWCNT fibres as efficient electron emitters with very high emission current for robust cold cathodes

V. Guglielmotti [a], E. Tamburri [a], S. Orlanducci [a], M.L. Terranova [a], M. Rossi [b,*], M. Notarianni [b], S.B. Fairchild [c], B. Maruyama [c], N. Behabtu [d], C.C. Young [d], M. Pasquali [d,e]

[a] Dip.to Scienze e Tecnologie Chimiche, Università degli Studi di Roma "Tor Vergata", Via della Ricerca Scientifica, 00133 Roma, Italy
[b] Dip.to di Scienze di Base e Applicate per l'Ingegneria, Università degli Studi di Roma "Sapienza", Via A. Scarpa, 00161 Roma, Italy
[c] Materials & Manufacturing Directorate, Air Force Research Laboratory, Wright-Patterson AFB, Dayton, OH, USA
[d] Department of Chemical & Biomolecular Engineering and Chemistry, Rice University, Houston, TX, USA
[e] The Smalley Institute for Nanoscale Science & Technology, Rice University, Houston, TX, USA

ARTICLE INFO

Article history:
Received 27 June 2012
Accepted 17 September 2012
Available online 25 September 2012

ABSTRACT

A novel of self-standing nanotube-based cold cathode is described. The electron emitter is a single macroscopic fibre spun from neat single wall carbon nanotubes and consists of an ensemble of nanotube bundles held together by van der Waals forces. Field emission measurements carried out using two different types of apparatus demonstrated the long working life of the realised cathode. The system is able to emit at very high current densities, up to 13 A/cm^2, and shows very low values of both turn on and threshold field, 0.12 V/μm and 0.21 V/μm, respectively. Such easy to handle self-standing electron sources assure good performances and represent an enabling technology for a scalable production of cold cathodes.

© 2012 Elsevier Ltd. All rights reserved.

1. Introduction

Due to a unique combination of properties, including high electrical and thermal conductivity, and high mechanical/chemical/thermal stability, carbon nanotubes (CNTs) have been recognised as ideal candidate materials for application in microelectronics [1]. Moreover, the high aspect ratio characterising this intriguing material makes possible to significantly strengthen electric fields into the vicinity of nanotubes tips. CNT-based materials generate high electron field emission (FE) currents at moderate voltages, supporting such currents for long times [2–8]. Field emission from carbon nanotubes is a hot point in science and applications of carbon nanostructures since about 2000 [9–11]. For all these reasons, nanotube-based cold cathodes are also foreseen to be effective for high power THz sources and amplifiers, which are expected to revolutionise the field of remote sensing and communication.

The achieving of the desired current densities using carbon nanotubes has always been problematic. The simple increasing of nanotubes density results in a screening of the electric field and mitigation of the benefit of the high aspect ratio. Some researchers have partially overcome such drawbacks by patterning carpets or films of nanotubes into discrete emitters [5,6]. However, the combination of high

* Corresponding author.
E-mail address: marcorossi@uniroma1.it (M. Rossi).
0008-6223/$ - see front matter © 2012 Elsevier Ltd. All rights reserved.
http://dx.doi.org/10.1016/j.carbon.2012.09.037

current density and durability has to date eluded nanotube field emitters.

At the same time, as the cathode area becomes larger to meet high current density, there is an increasing need for beam focusing by electrostatic or magnetic lenses. On the other hand, this apparently inevitable setup integration undermines the required compactness for some vacuum electronic devices, such as X-ray sources for imaging and high frequency travelling wave tube amplifiers [12,13]. An enabling solution could be the use of small diameter cathodes emitting high current densities, such as microribbons of self-assembled CNT bundles [14,15] or fibres [16,17] made by aligned CNT bundles. The cross sectional area of these macroscopic point emitters could be engineered in order to meet the current requirements. In this context, an increasing interest is being given to the issue of preparing CNT-based fibres and yarns, as indicated by several investigations in the last few years [18–23].

Two main approaches have emerged for the production of neat carbon nanotube fibres: the dry and the liquid-state spinning process [23]. Both approaches attain continuous spinning. However the liquid state spinning is intrinsically more scalable than the solid-state one. The main difference between them stems from the ability of the liquid state spinning to modify the CNT morphology. One of these liquid state processes is the superacid spinning developed by Ericson et al. [24].

Superacids are the only known solvents for carbon nanotubes [25,26] and allow the formation of a liquid crystalline phase. Superacid spinning produces fibres characterised by a density and an alignment which are higher than those obtained for the solid-state spun fibres. An added value for FE applications is represented by the high values of thermal and electrical conductivity, typical of the nanotubes, and still retained by the fibres [27].

In the present research, we have addressed the task of studying the field emission properties of small diameter (<100 μm) single fibre-based cathodes made by superacid spinning of single wall carbon nanotubes (SWCNTs). The technical challenge was to test a new type of self-standing, easy manipulating cathode able to generate the small diameter high current electron beams required for high power sources and travelling wave tube amplifiers.

2. Experimental details

Macroscopic neat SWCNT fibres are produced following our established methodology [24]. Starting from purified HiPco SWCNT powders containing less than 1 wt% residual metal catalyst, 108% sulfuric acid is added to dry SWCNT powder to obtain an 8 wt% SWCNT solution in an anhydrous glove box (dew point −50 °C). The SWCNT/acid solution (called dope hereafter) is typically extruded at 1.5 m/min in a static water coagulation bath using a syringe. Water extracts the acid leaving behind a solid fibre. Polyvinyl alcohol (PVA) (3000 Mw) is also dissolved up to 1 wt% in the coagulation bath to slow down coagulation and improve fibre tensile strength. The amount of added PVA is not significant and does not considerably affect the fibre electrical conductivity [27]. The fibre is then collected on wheels and dried at 110 °C. Various fibre diameters can be obtained by spinning from different spinneret size. For the present experiments, fibres with a diameter less than 100 μm were prepared. For the characterizations, several 6 mm long segments were obtained by mechanical (razor blade) cutting. The morphological characterizations of the fibres were carried out by scanning electron microscopy (SEM).

Field emission measurements were performed in a diode configuration, using two different types of apparatus. Overall the emission current was measured as a function of the applied voltage in a range 500–2000 V. The anode–cathode distance (A–C), *i.e.* the distance of the fibre tip (cathode) from the collecting anode, was varied from 270 micrometres up to 5 millimetres.

Some measurements were carried out using the custom-designed apparatus installed in the “Tor Vergata” labs, and following the methodology settled by Boscolo et al. [28], according to which the evaluation of anode–cathode distance has been made via the measurement of the anode–cathode capacitance. The accuracy in the distance determination is 1 μm. In this experiments a cylindrical Al anode (diameter: 6 mm) was used, and the chamber operating pressure was of 1×10^{-8} Torr. The fibres were tested in a free-standing geometry by attaching one end to a flat plate with a conductive tape.

Further measurements were performed at AFRL by using the following set up. A moveable anode consisting of a 3 mm diameter oxygen-free high thermal conductivity (OFHC) copper cylinder tapered to a 750 μm diameter end is mounted on an integrated motor stepper (IMS) providing 2.5 μm step size for accurate anode–cathode gap spacing. The chamber vacuum was typically of 2×10^{-8} Torr. Even though the geometries of the FE systems at “Tor Vergata” University and AFRL were different, similar emission data from the SWCNT fibres were achieved for the same A-C distances using the two different type of apparatus.

3. Results and discussion

A fibre segment protruding from a circular holder is reported in the SEM image of Fig. 1a. The fibres are formed by a network of nanotubes bundles held together along the same direction by van der Waals forces. More details of a typical top section obtained by mechanically cutting down the fibres (by a razor) are shown in Fig. 1b and c.

Emission experiments were carried out at voltages in the range 500–2000 V for A–C distances of 5, 3 and 1 mm, and in the range 500–1000 V for A–C distances of 500, 350 and 270 μm. In this last case, we have been forced to reduce the voltage range because at values higher than 1000 V relevant spikes and electrical discharges were found to occur.

In Fig. 2a and b we reported the trend of the field emission current (I) versus the applied voltage (V), detected by the two measurements setups for the larger and the closer (A–C) distances, respectively. In addition, on the right part of the *I/V* curves the corresponding Fowler–Nordheim (FN) plots and the current versus electric field (*I/E*) are shown [29].

Each measurement was repeated sweeping the voltage up and down, in order to confirm the reproducibility of the field emission process.

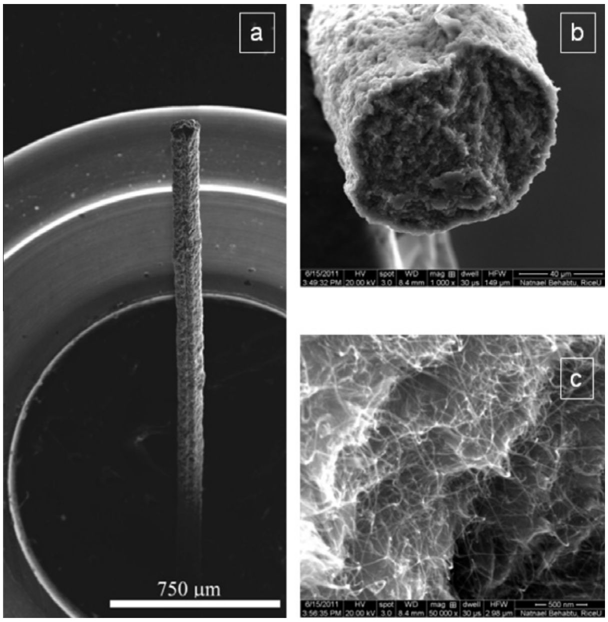

Fig. 1 – SEM images of a SWCNT fibre: (a) general view of the fibre fixed on the SEM circular holder; (b) and (c) top section view of the fibre with details.

A preliminary conditioning step, carried out by the application of a moderate electrical field, has been demonstrated to be a key factor in order to achieve a stable emission for cathodes made of pure CNT [30–32]. Further approaches consisting of coating CNTs with wide band gap materials have been proposed and in the case of CNT/diamond hybrid systems, for instance, the effective work function and the turn-on field for the electron emission are expected to be reduced [33–36].

The emission stabilization is due to the out-gassing of loosely bound adsorbates from the emitters, and the rearrangements of the strongly bound ones in a stable energetic configuration of the emitters, with consequent stabilization of the work function values.

Conversely, in the case of SWCNT fibre systems, *I/V* sweeps performed during the data acquisition sessions demonstrated a stable and reproducible current emission, even from the beginning, without the need of the pre-conditioning procedure.

The *I/V* curves reported in Fig. 2a evidence that, by reducing the A–C distance from 5 mm to 1 mm, one finds that the currents collected by the anode reach the value of 1 mA at 2000 V, *i.e.* one order of magnitude higher than the value (100 μA) obtained for A–C distances of 5 mm and 3 mm. The measurements carried out reducing the A–C distances to 500, 350 and 270 μm indicate a further increase of the emission that at 1000 V reaches the value of 300 μA (Fig. 2b).

In the case of A–C distances shorter than 1 mm, it was not possible to perform measurements at voltages higher than 1000 V because of the occurrence of arc discharges during the sweep-on of the voltage.

Current density has been estimated from *I/V* data by considering the geometrical area of the fibre top section, as evaluated from the FE-SEM images. Nevertheless a slight underestimation of the real emitting area is probably made using this approach because of the CNT protruding the top end fibre. It is to be noted that the maximum value of current density evaluated for the SWCNT fibres is about 13 A/cm^2 at 2000 V, with an A–C distance of 1 mm.

A particularly compelling feature of the field emission from such fibres is the low value of both turn-on and threshold field, defined as the applied electric field necessary to collect 1 nA and 1 μA of the emitted current, respectively. From all the measurements performed as a function of the distance from the fibre tip to the anode, we found the lowest turn-on and threshold values of 0.12 and 0.21 V/μm respectively, with average values of 0.73 and 1.1 V/μm. These values match remarkably closely the best literature data reported for turn-on and threshold fields of some CNT types [5,44,37]. Clearly a reduction of the applied field, due to low values of both turn-on and threshold, decreases the likelihood of the emitter's failure and provides an excellent potential for working in high current regimes [38,39].

The field emission data have been analysed in the frame of the FN model, following an already established procedure. The FN plots obtained from the various *I/V* curves are reported in Fig. 2a_i and b_i. According to the FN equation [29], the slope of the curves is proportional to $-\varphi^{3/2}d/\beta$ where φ is the work function of the emitter, d is the A–C distance and β is the field amplification factor. The β factor, mostly determined by the geometrical shape of the emitter, reflects the ability of the emitter to concentrate the applied electric field E.

As representative results of the experimental procedure adopted to characterise the field emission behaviour of the fibre, in Fig. 3a we report the best fit obtained in the central linear region for a set of FN plots. Such graphs correspond to the *I/V* curves collected for a predefined A–C distance. In Fig. 3b is also reported the emission stability measured by applying a constant potential difference between anode and cathode. Fig. 3a confirms the trend already noted in Fig. 2.

By focusing attention on the obtained FN plots (see Fig. 2a_i and b_i), deviations from the FN theoretical behaviour are detected.

In Fig. 4a and b these FN plots for both millimetre and micrometre A–C ranges are highlighted.

The origin of the deviation from the FN plot at high field region has been long argued. Several mechanisms have been proposed. One of the commonly referenced models is a space charge effect [40,41]. The change of the slope at high field could be induced by the space charges between two electrodes, and suppress the emission currents by screening the electric field near the emitters [42]. There is the possibility that tip–tip interactions may suppress the emission due to screening effects [43].

Localised defect states, which are observed at the apex of the CNT, may also be the cause of the saturation phenomenon. Moreover, the gas adsorbates introduced during the fabrication process are a good candidate for the origin of the current suppression [44].

In our case, the deviation from FN law seems to be better explained by using the approach reported by Zakhidov et al. [20], according to which the plot can be split into three regions, each one characterised by a different field emission behaviour [45,46]. At lowest voltages (range I) – no FE current

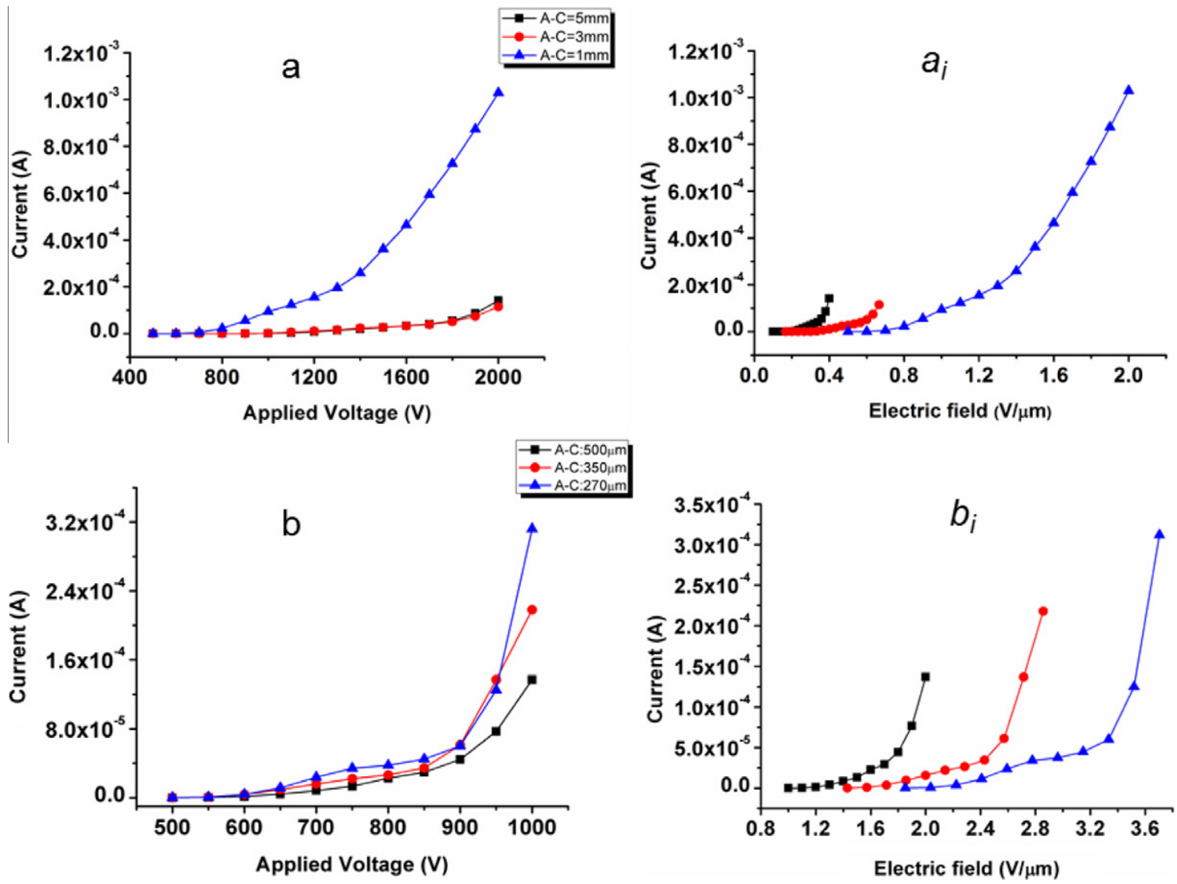

Fig. 2 – I/V curves of the SWCNT fibre: (a) larger A–C distances; (b) closer A–C distances; with the corresponding current versus electric field plots in a_i and b_i, respectively.

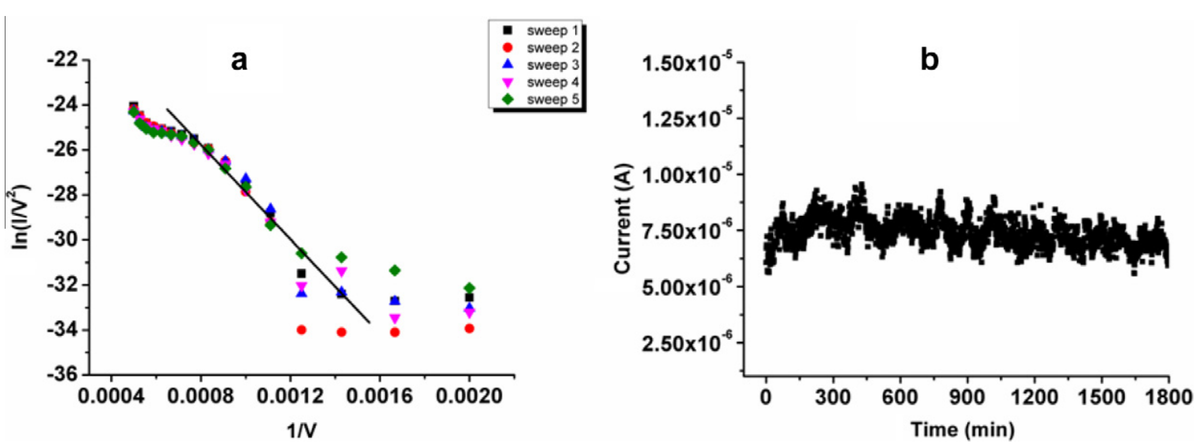

Fig. 3 – (a) Fowler–Nordheim plots from multiple I/V sweeps; (b) emission stability of the fibre.

except noise is detected. In the range II, the emission obeys to the FN law [47], and the field enhancement factor from the slope of the rough lines which pass among the points can be estimated. In the range III, the FE *I/V* curve deviates from FN law. Such trend is attributed to the current saturation due to the local Joule heating of emitting SWCNT species on the top of the fibre [48]. This heating likely cause extensive desorption of molecules from nanotubes, thus eliminating the adsorbate-enhanced field emission mechanism [49], or just an additional voltage drop due to conductance decrease of the tubes. Above a certain FE current value, this local Joule heating also leads to vacuum breakdown of SWCNT [50]. In conclusion, it is reasonably to consider that the real mechanism to emit electrons followed by the SWCNT fibres-based cathodes can be correctly explained by considering this “three range” plot.

On the basis of these considerations, the β factor for the SWCNT fibres has been calculated from the slope of the FN

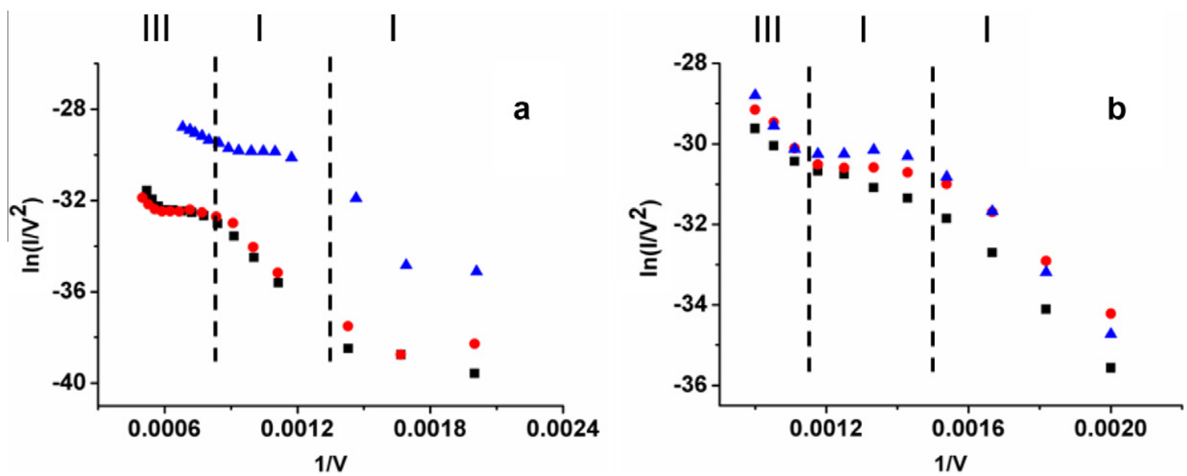

Fig. 4 – Fowler–Nordheim plots: (a) millimetre range A–C distances; (b) micrometre range A–C distances.

plots in the current region II, under the assumption that the work function of the SWCNT is the same as that of graphite or C60 (5 eV). From all the *I/V* curves measured at the various A–C distances, we observed that by varying the A–C distance from μm to mm range, the β factor increases by 1 order of magnitude up to reach the highest value of 6.5×10^4. Such value is among the largest reported so far [5].

Such a high β value can be rationalised considering the main factors contributing to the field emission behaviour of carbon nanotube arrays, *i.e.* morphology, diameter, alignment as well as defects, adsorption, open or capped end and so on. In particular, the structure of the fibre tops, and the specific features of the nanotubes protruding from the cross-sectioned segments represent a further key factor which can affect the FE characteristics. The field emission characteristics of the side of a multi wall carbon nanotube (MWCNT) loop have been measured and compared with those of the tip of a MWCNT under the same experimental conditions as largely discussed in [51]. Other authors reported a study regarding the realisation of cold cathodes using MWCNT yarns. These systems were considered to be a good candidate for field emitters because their tip structure resembles the typical structure of the emitter. In particular, as described by Jang et al. [52], the difference between the emission properties from the tip and the side of MWCNT yarns was investigated.

In this context, it has been already stated that the open-ended nanotubes may generate a higher field amplification effect with respect to the closed ones, resulting in electron emission at lower fields [9,53,54]. This is because the irregularly shaped graphitic sheets at the tip of open-ended nanotubes have circular sharp edges with a radius of curvature smaller than the closed-ended nanotubes, and can likely assist in enhancing the field amplification effect. The cutting procedures used to section the fibres in the smaller segments may have played a relevant role in generating such favourable emission condition.

4. Conclusions

A study of the field emission from macroscopic fibres formed by purified HiPco SWCNT has been performed in a diode configuration using a vertical free-end geometry. The fibres, produced by assembling nanotube bundles extruded from superacid suspensions into a coagulant (water), represent a novel type of self-standing and easily handled SWCNT-based cathodes. The lateral packing of the nanotube-based subunits in compact and robust fibres is achieved without the need of any external support. The lack of foreign species meets the requirements for advantageous applications of these fibres in vacuum electronics.

Many prominent emitting features characterise the fibres (less than 100 μm in diameter) produced in the present experiments. First of all, one must consider the high field enhancement factor of 6.5×10^4, that governs the values of the turn-on and threshold field, found at about 0.12 and 0.21 V/μm, respectively. Other outstanding features include very high current densities up to 13 A/cm^2 (considering the emitting surface area of the investigated fibres), at 2000 V, no need of pre-conditioning procedures and no hysteresis after repeated up/down scans. The lifetime tests indicated robust stability of the emission over long-lasting measurement cycles.

The performances of these fibres enable to devise the fabrication of micron scale electron sources and the design of a multi-beam system with each cathode sending a small diameter, high current electron beam to its corresponding focal point. Whereas the task of assembling cathodes for small beam tunnels using CNT bundles located on a predefined pattern is quite challenging, the already settled processing technique for the fabrication on an industrial scale of macroscopic fibres allows one to overcome the principal difficulty associated with the nanotube application, *i.e.* an efficient manufacturing and handling method.

Not only high power devices could take advantage of these single fibre cold cathodes. As an example, non-destructive inspection of LSI circuit patterns, too fine to be resolved with conventional X-rays, could be performed using miniaturised X-ray tubes based on electron emitting fibres. Our next concern will be to fabricate an array of SWCNT fibres that are individually addressable via an electronic circuit. Such free-standing and self-standing macroscopic cold cathodes easy to handle and scale up, appear to be an enabling technology ready for the rapid development of a new class of electron emitters.

Acknowledgments

This work was supported by AFOSR (FA9550-06-1-0207 & FA9550-09-1-0590), AFRL (FA8650-07-2-5061 & 07-S568-0042-01-C1), and the Welch Foundation (C-1668).

REFERENCES

[1] Kreupl F. Carbon nanotubes in microelectronic applications. In: Hierold C, editor. Carbon nanotube devices: properties, modeling, integration and applications. Advanced micro & nanosystems, vol. 8. Winheim: Wiley-VCH; 2008. p. 1–41.
[2] Chernozatonskii LA, Gulyaev YuV, Kosakovskaja ZJa, Sinitsyn NI, Torgashov GV, Zakharchenko YuF, et al. Electron field emission from nanofilament carbon films. Chem Phys Lett 1995;233:63–8.
[3] Rinzler AG, Hafner JH, Nikolaev P, Nordlander P, Colbert DT, Smalley RE, et al. Unraveling nanotubes: field emission from an atomic wire. Science 1995;269:1550–3.
[4] Eletskii AV. Carbon nanotube-based electron field emitters. Phys Usp 2010;53:863–92.
[5] Perea-López N, Rebollo-Plata B, Briones-León JA, Morelos-Gómez A, Hernández-Cruz D, Hirata GA, et al. Millimeter-long carbon nanotubes: outstanding electron-emitting sources. ACS Nano 2011;5:5072–7.
[6] Yun J, Wang R, Choi WK, Thong JTL, Thompson CV, Zhu M, et al. Field emission from a large area of vertically-aligned carbon nanofibres with nanoscale tips and controlled spatial geometry. Carbon 2010;48:1362–8.
[7] Calderón-Colón X, Geng H, Gao B, An L, Cao G, Zhou O. A carbon nanotube field emission cathode with high current density and long-term stability. Nanotechnology 2009;20:325707–11.
[8] Baughman RH, Zakhidov AA, de Heer WA. Carbon nanotubes – the route toward applications. Science 2002;297:787–92.
[9] Saito Y, Uemura S. Field emission from carbon nanotubes and its application to electron sources. Carbon 2000;38:169–82.
[10] De Jonge N, Bonard JM. Carbon nanotube electron sources and applications. Philos Trans R Soc London A 2004;362:2239–66.
[11] Chai G, Chow L. Electron emission from the side wall of an individual multiwall carbon nanotube. Carbon 2007;45: 281–4.
[12] Lee YZ, Burk L, Wang K, Cao G, Lu J, Zhou O. Carbon nanotube based X-ray sources: applications in pre-clinical and medical imaging. Nucl Instrum Methods Phys Res A 2011;648:S281–3.
[13] Choi HY, Shon CH, Kim JU. Development of new X-ray source based on carbon nanotube field emission and application to the non destructive imaging technology. IEEE Trans Nucl Sci 2009;56:1297–300.
[14] Serra A, Manno D, Filippo E, Tepore E, Terranova ML, Orlanducci S, et al. Photoconductivity of packed homotype bundles formed by aligned single-walled carbon nanotubes. Nano Lett 2008;8:968–71.
[15] Xu F, Wang X, Zhu Y, Zhu Y. Wavy ribbons of carbon nanotubes for stretchable conductors. Adv Funct Mater 2012;22:1279–83.
[16] Shiffler D, Fairchild S, Tang W, Maruyama B, Golby K, LaCour M, et al. Demonstration of an acid-spun single-walled nanotube fibre cathode. IEEE Trans Plasma Sci 2012;40:1871–7.
[17] Lee J, Jung Y, Song J, Kim JS, Lee G-W, Jeong HJ, et al. High-performance field emission from a carbon nanotube carpet. Carbon 2012;50:3889–96.
[18] Wei Y, Weng D, Yang Y, Zhang X, Jiang K, Liu L, et al. Efficient fabrication of field electron emitters from the multiwalled carbon nanotube yarns. Appl Phys Lett 2006;89:063101–2.
[19] Zhang S, Koziol KKK, Kinloch IA, Windle AH. Macroscopic fibres of well-aligned carbon nanotubes by wet spinning. Small 2008;4:1217–22.
[20] Zakhidov ALA, Nanjundaswamy R, Obraztsov AN, Zhang M, Fang S, Klesh VI, et al. Appl Phys A 2007;88:593–600.
[21] Vilatela JJ, Windle AH. Yarn-like carbon nanotube fibres. Adv Mater 2010;22:4959–63.
[22] Chen G, Shin DH, Roth S, Lee CJ. Field emission characteristics of point emitters fabricated by a multiwalled carbon nanotube yarn. Nanotechnology 2009;20:315201–5.
[23] Behabtu N, Green MJ, Pasquali M. Carbon nanotube-based neat fibres. Nano Today 2008;3:24–34.
[24] Ericson LM, Fan H, Peng H, Davis VA, Zhou W, Sulpizio J, et al. Macroscopic, neat, single-walled carbon nanotube fibres. Science 2004;305:1447–50.
[25] Davis VA, Parra-Vasquez ANG, Green MJ, Rai PK, Behabtu N, Prieto V, et al. True solutions of single-walled carbon nanotubes for assembly into macroscopic materials. Nat Nanotech 2009;4:830–4.
[26] Parra-Vasquez ANG, Behabtu N, Green MJ, Pint CL, Young CC, Schmidt J, et al. Spontaneous dissolution of ultralong single- and multiwalled carbon nanotubes. ACS Nano 2010;4:3969–78.
[27] Zhou W, Vavro J, Guthy C, Winey KI, Fischer JE, Ericson LM, et al. Single wall carbon nanotube fibres extruded from super-acid suspensions: preferred orientation, electrical, and thermal transport. J Appl Phys 2004;95:649–55.
[28] Boscolo I, Cialdi S, Fiori A, Orlanducci S, Sessa V, Terranova ML, et al. Capacitive and analytical approaches for the analysis of field emission from carbon nanotubes in a sphere-to-plane diode. J Vac Sci Technol B 2007;25:1253–60.
[29] Nordheim LW. The effect of the image force on the emission and reflexion of electrons by metals. Proc R Soc London A 1928;121:626–39.
[30] Dean KA, Chalamala BR. Current saturation mechanisms in carbon nanotube field emitters. Appl Phys Lett 2000;76:375–7.
[31] Angelucci R, Boscolo I, Ciorba A, Cuffiani M, Malferrari L, Montanari A, et al. Honeycomb arrays of carbon nanotubes in alumina templates for field emission based devices and electron sources. Physica E 2010;42:1469–76.
[32] Dong C, Gupta MC. Influences of the surface reactions on the field emission from multiwall carbon nanotubes. Appl Phys Lett 2003;83:159–61.
[33] Guglielmotti V, Chieppa S, Orlanducci S, Tamburri E, Toschi F, Terranova ML, et al. Carbon nanotube/nanodiamond structures: an innovative concept for stable and ready-to-start electron emitters. Appl Phys Lett 2009;95:222113–5.
[34] Barnard AS, Terranova ML, Rossi M. Density functional study of H-induced defects as nucleation sites in hybrid carbon nanomaterials. Chem Mater 2005;17:527–36.
[35] Vul' AYa, Reich KV, Eidelman ED, Terranova ML, Orlanducci S, Sessa V, et al. A model of field emission from carbon nanotubes decorated by nanodiamonds. Adv Sci Lett 2010;2:110–6.
[36] Cui T, Lv R, Kang F, Hu Q, Gu J, Wang K, et al. Synthesis and enhanced field-emission of thin-walled, open-ended, and well-aligned N-doped carbon nanotubes. Nanoscale Res Lett 2010;5:941–8.
[37] Hazra KS, Rai PK, Mohapatra DR, Kulshrestha N, Bajpai R, Roy S, et al. Dramatic enhancement of the emission current density from carbon nanotube based nanosize tips with extremely low onset fields. ACS Nano 2009;3:2617–22.
[38] Wei W, Jiang K, Wei Y, Liu M, Yang H, Zhang L, et al. Measuring the stress in field-emitting carbon nanotubes. Nanotechnology 2006;17:1994–8.

[39] Wang ZL, Gao RP, de Heer WA, Poncharal P. In situ imaging of field emission from individual carbon nanotubes and their structural damage. Appl Phys Lett 2002;80:856–8.
[40] Bonard JM, Maier F, Stockli T, De Heer WA, Chatelain A, Salvetat JP, et al. Field emission properties of multiwalled carbon nanotubes. Ultramicroscopy 1998;73:7–15.
[41] Dimitrijevic S, Withers JC, Mammana VP, Monteiro OR, Ager JW, Brown IG. Electron emission from films of carbon nanotubes and ta-C coated nanotubes. Appl Phys Lett 1999;75:2680–3.
[42] Schwoebel PR, Brodie I. Surface-science aspects of vacuum microelectronics. J Vac Sci Technol B 1995;13:1391–411.
[43] Collins PG, Zettle A. Unique characteristics of cold cathode carbon-nanotube-matrix field emitters. Phys Rev B 1997;55:9391–9.
[44] Chen Y, Deng SZ, Xu NS, Chen J, Ma XC, Wang EG. Physical origin of non-linearity in Fowler–Nordheim plots of aligned large area multi-walled nitrogen-containing carbon nanotubes. Mater Sci Eng A 2002;A327:16–9.
[45] Choi YC, Shin YM, Bae DJ, Lim SC, Lee YH, Lee BS. Patterned growth and field emission properties of vertically aligned carbon nanotubes. Diamond Relat Mater 2001;10:1457–64.
[46] Chung MS, Yoon BG. Analysis of the slope of the Fowler–Nordheim plot for field emission from n-type semiconductors. J Vac Sci Technol B 2003;21:548–51.
[47] Gomer R. Field emission and field ionization. Cambridge: Harvard University Press; 1961.
[48] Purcell ST, Vincent P, Journet C, Binh VT. Hot nanotubes: stable heating of individual multiwall carbon nanotubes to 2000 K induced by the field-emission current. Phys Rev Lett 2002;88:105502–5.
[49] Saito R, Fujita M, Dresselhaus G, Dresselhaus MS. Electronic structure of chiral graphene tubules. Appl Phys Lett 1992;60:2204–6.
[50] Huang NY, She JC, Chen J, Deng SZ, Xu NS, Bishop H, et al. Mechanism responsible for initiating carbon nanotube vacuum breakdown. Phys Rev Lett 2004;93:075501–4.
[51] Konishi Y, Hokushin S, Tanaka H, Pan L, Akita S, Nakayama Y. Comparison of field emissions from side wall and tip of an individual carbon nanotube. Jpn J Appl Phys 2005;44:1648–51.
[52] Jang HS, Jeon SK, Nahm SH. Field emission properties from the tip and side of multi-walled carbon nanotube yarns. Carbon 2010;48:4019–23.
[53] Lv R, Kang F, Zhu D, Zhu Y, Gui X, Wei J, et al. Enhanced field emission of open-ended, thin-walled carbon nanotubes filled with ferromagnetic nanowires. Carbon 2009;47:2709–15.
[54] Wang MS, Peng LM, Wang JY, Jin CH, Chen Q. Quantitative analysis of electron field-emission characteristics of individual carbon nanotubes: the importance of the tip structure. J Phys Chem B 2006;110:9397–402.